Passive Scalar Function Approximation Using SOS Polynomials

Arif Ege Engin, *Member, IEEE*

***Abstract*—Signal and power integrity design in the time domain requires equivalent circuit models for interconnects and packages, whose descriptions may only be available as tabulated impedance or admittance parameters. Accurate models for these components should maintain their physical properties including causality, stability, and passivity. Even though a heuristic approach, pole flipping (i.e., changing the sign of the real part of an unstable pole) has proven to be sufficiently accurate for many applications, resulting in models with ensured causality and stability. In this article, we address the problem of generating passive scalar models, such as driving point impedances or admittances, based on an existing causal, stable, but nonpassive model. Our approach is based on using sum-of-squares (SOS) polynomials and results in a convex optimization problem, hence a global optimum is obtained. We obtain approximations through two distinct SOS algorithms: a coefficient and a sampling-based method. We also present a simple passivity test for such functions based on calculating the roots of numerator and denominator polynomials, which provides an intuitive link among existing approaches based on solving an eigenvalue problem.**

***Index Terms*—Causality, macromodeling, passivity, rational function, stability, sum-of-squares (SOS), transfer function, vector fitting.**

I. Introduction

MACROMODELING of passive networks from tabulated simulated or measured data is a critical step in signal and power integrity design. Macromodeling involves approximating the given data with a rational transfer function, which can then be converted to an equivalent circuit model for time-domain simulation. Available methods for rational transfer function approximation include vector fitting [1], Loewner framework [2], Sanathanan–Koerner iteration [3], and adaptive Antoulas–Anderson (AAA) [4], [5]. For signal and power integrity analysis, the vector fitting algorithm in particular has been applied with success on many applications. An alternative to macromodeling is using the raw data in time-domain simulation based on a convolution approach [6]. The raw data may, however, be flawed with causality violations, which may be difficult to identify and fix [7].

Manuscript received June 7, 2021; revised October 27, 2021 and December 13, 2021; accepted December 30, 2021. *(Corresponding author: Arif Ege Engin.)*

The author is with the Department of Electrical and Computer Engineering, San Diego State University, San Diego, CA 92182 USA (e-mail: aengin@sdsu.edu).

Color versions of one or more figures in this article are available at https://doi.org/10.1109/TEMC.2021.3140198.

Digital Object Identifier 10.1109/TEMC.2021.3140198

In this article, we address the problem of generating passive scalar models for driving point impedances or admittances, based on an existing causal, stable, but nonpassive model. Even though a stable rational function approximation may provide an excellent fit to the provided passive data, it may still be nonpassive due to passivity violations outside of the frequency range of approximation or even between consecutive frequency points of approximation. Moreover, measured or simulated data may itself be nonpassive due to measurement noise or modeling issues. A passivity violation occurs in a macromodel when the real part of such a rational function becomes negative. To correct for passivity violations, existing methods available to enforce passivity of the model include iterative perturbation of residues [8] or Hamiltonian matrices [9], [10], and fitting using positive fractions or linear matrix inequalities [11]–[13].

We start with presenting a simple passivity test for such scalar rational functions based on calculating the roots of numerator and denominator polynomials, which can be more intuitive than the common eigenvalue-problem-based approach. Based on this simple test, we introduce our approach for ensuring passivity based on using sum-of-squares (SOS) polynomials. We fit the residues to obtain a passive model by solving a convex optimization problem, hence a global optimum can be obtained after convergence.

II. Passivity Test for Scalar Functions Based on Their Roots

Assume that the scalar transfer function for a driving-point impedance or admittance is given as a rational function or in an equivalent pole-residue form as

$$r(s) = \frac{\sum_{i=0}^{M} a_i s^i}{\sum_{i=0}^{N} b_i s^i} = d + se + \sum_{i=0}^{N} \frac{k_i}{s - p_i}. \quad (1)$$

This rational function will be passive if the following conditions hold [14].

1) The coefficients a_i, b_i are real (i.e., $r^*(s) = r(s^*)$).
2) All poles p_i are stable, that is they do not have positive real parts. If there are any pure imaginary poles, they should be simple and have positive residues (including the residue e of the pole at infinity).
3) The real part of the rational function is nonnegative at all real frequencies $s = j\omega$ (i.e., $r(j\omega) + r^*(j\omega) \geq 0$).

Standard macromodeling algorithms can ensure the first two conditions by enforcing real coefficients and pole flipping. Considering that possible poles at 0 and at infinity should be simple, the second requirement also limits the degree of the polynomials such that $|N - M| \leq 1$. It is not possible to test for the third condition by a frequency sweep, since passivity violations between or outside the range of tested frequency samples will not be detected.

The even part $r_e(s) = (r(s) + r(-s))/2$ of $r(s)$ can be obtained from its pole-residue form as

$$r_e(s) = d + \frac{1}{2}\sum_{i=0}^{N}\left(\frac{k_i}{s - p_i} + \frac{k_i}{-s - p_i}\right)$$
$$= d + \sum_{i=0}^{N}\frac{k_i p_i}{s^2 - p_i^2} \quad (2)$$

which allows to obtain the real part of $r(j\omega)$ from $r_e(s)$ at $s = j\omega$ as

$$\frac{r(j\omega) + r^*(j\omega)}{2} = d + \sum_{i=0}^{N}\frac{-k_i p_i}{\omega^2 + p_i^2} = \frac{n(\omega^2)}{d(\omega^2)}. \quad (3)$$

Theorem 1: A scalar rational function with real coefficients and stable poles (including simple pure imaginary poles with positive residues) will be passive if the real part numerator polynomial $n(\omega^2)$ in (3) has no positive real roots of odd multiplicity. The square root of any such root provides a frequency point where a passivity violation begins or ends.

Proof: We do not need to consider any pure imaginary poles in the summation of (3) as any such pole has a real residue and does not contribute to the real part of $r(j\omega)$. We can then observe that the denominator polynomial does not cross the ω-axis (i.e., it has no real roots), therefore $d(\omega^2) > 0$. For the rational function to be passive, then the numerator polynomial should be nonnegative, or $n(\omega^2) \geq 0$ for all ω. This allows us to check for passivity by calculating the roots of $n(\omega^2)$. The real part of $r(j\omega)$ would change sign at any positive real root with odd multiplicity, indicating a frequency point where a passivity violation begins or ends. □

As an example consider the transfer function

$$r(s) = 0.8 + \frac{-1 + 2j}{s - (-1 - j)} + \frac{-1 - 2j}{s - (-1 + j)} + \frac{1}{s - (-1)}. \quad (4)$$

The polynomial $n(\omega^2)$ has two real roots at $\omega = 1.61, 2$. This rational function is not passive since its real part will change sign at these two frequencies.

A. Relationship to State-Space Passivity Tests

Next, we discuss the relationship of the presented method to passivity tests based on the state-space form of the network given as

$$\dot{x} = Ax + bu \quad (5)$$

$$y = c^T x + du \quad (6)$$

which corresponds to the transfer function $r(s) = c^T(sI - A)^{-1}b + d$. The third passivity condition can be replaced with the condition that the test matrix T, obtained by

$$T = (bd^{-1}c^T - A)A \quad (7)$$

should have no positive-real eigenvalues. If it does, then the square-root of the positive-real eigenvalues are the frequencies where passivity violations start or end [15]. We can observe that the T matrix indeed gives the roots of $n(\omega^2)$, based on the eigenvalue method for calculating the zeros of a rational function in pole-residue form as it is used in relaxed vector fitting [16].

This passivity test requires that d is nonzero. For the case with $d = 0$, a different test matrix is used in [17]

$$\hat{T} = A\left[(1/c^T Ab)Abc^T - I\right]A \quad (8)$$

which is equivalent to finding the zeros of the real part from the pole-residue form of (3) when $d = 0$ [18].

The presented test is intuitive as it is based on finding the roots of a polynomial only and equivalent to the state-space tests. This test provides a link between separate passivity tests applied based on the presence of a constant term d in the pole-residue form.

III. Passivity Test Using SOS Polynomials

Theorem 1 shows that a requirement for passivity is that $n(\omega^2)$ is a positive semidefinite (PSD) polynomial (i.e., $n(\omega^2) \geq 0$ for all ω.) It is well known that such a univariate polynomial is PSD if and only if it is a SOS polynomial given by

$$n(\omega^2) = \sum_{i=0}^{k} m_i(\omega)^2 \quad (9)$$

where the degree of each polynomial m_i is smaller than or equal to $(N + 1)$ [19]. For a PSD polynomial, there is always a decomposition with $k + 1 = 2$ terms, but in general there may be multiple possible decompositions.

One way to test whether a univariate polynomial is PSD is through the Gram matrix Q of the SOS representation

$$n(\omega^2) = [\omega]^T Q[\omega], \quad Q \succeq 0 \quad (10)$$

where Q is a symmetric PSD matrix, and the monomial vector is given as $[\omega]^T = [1, \omega, \ldots, \omega^{N+1}]$. This allows us to solve the problem using a semidefinite program; a feasible solution for a PSD Q proves that $n(\omega^2)$ is a PSD polynomial. The semidefinite program searches for a PSD Q subject to the equality constraints of the polynomial coefficients on both sides of (10) as

$$n_k = \sum_{i+j=k} Q_{ij}, \quad k = 0, 1, \ldots, 2(N + 1) \quad (11)$$

where $n(\omega^2) = \sum_{k=0}^{2(N+1)} n_k\omega^k$, and the matrix Q is indexed so its elements are Q_{ij} where $i, j = 0, 1, \ldots, N + 1$.

In (11), all coefficients n_k with odd index will be zero since the polynomial is a function of ω^2. We can improve the efficiency of the semidefinite program by formulating it more precisely as a search for $n(\omega^2) \geq 0$ for all $\omega^2 \geq 0$, which can be expressed in terms of two SOS polynomials. More generally, $n(\omega^2)$ is PSD for all $\omega^2 \geq a$ [20], if and only if it can be expressed as

$$n(\omega^2) = \sum_{i=0}^{k_p} m_i^p(\omega^2)^2 + (\omega^2 - a)\sum_{i=0}^{k_r} m_i^r(\omega^2)^2. \quad (12)$$

This property allows to reformulate the semidefinite program using two smaller PSD matrices and expressing all polynomials as functions of ω^2 as

$$n(\omega^2) = [\omega^2]_p^T P [\omega^2]_p + \omega^2 [\omega^2]_r^T R [\omega^2]_r$$
$$P \succeq 0, R \succeq 0 \tag{13}$$

where $[\omega^2]_p^T = [1, \omega^2, \dots, \omega^{2p}]$, $[\omega^2]_r^T = [1, \omega^2, \dots, \omega^{2r}]$, P is a $(p+1) \times (p+1)$ symmetric matrix, and R is a $(r+1) \times (r+1)$ symmetric matrix. The size of the matrices depend on whether N is odd or even. For even N we get $p = r = N/2$; whereas for odd N we get $p = (N+1)/2, r = (N+1)/2 - 1$. A similar reduction in size can also be achieved by separating the even and odd basis polynomials as in [21] that suggests a significant gain in computational complexity.

IV. Approximation Using SOS Polynomials

The advantage of the approach in (13) over state-space based tests is that now we can solve a semidefinite program in least squares fitting of the residues of a rational function subject to its real part being PSD, or with guaranteed passivity. This is a norm minimization problem with PSD constraints given as

$$\begin{aligned} &\text{minimize} \quad \sum_{m=0}^{M} \left| d + j\omega_m e + \sum_{i=0}^{N} \frac{k_i}{j\omega_m - p_i} - h(j\omega_m) \right|^2 \\ &\text{subject to} \quad n(\omega^2) \geq 0 \quad \text{for } \omega^2 \geq 0, \quad e \geq 0 \end{aligned} \tag{14}$$

where $h(j\omega_m)$ is the provided impedance or admittance data at $M+1$ frequency points. In (14), the variables d and e are real and nonnegative, whereas residues k_i associated with complex poles can be complex but they should come in complex conjugate pairs. This can be achieved by the well-known modification of separating the real and imaginary parts of complex residues in the system matrix as applied in vector fitting [1]. The new aspect of (14) is the PSD constraint that is formulated as an SOS problem in (13). The coefficients of $n(\omega^2)$ can be obtained with an affine transformation from the variables d, k_i, (e.g., using an algorithm similar to the `residue` function in MATLAB) so we obtain a convex minimization problem, hence a global optimum can be obtained after convergence. We solve this problem using the CVX package [22]. This algorithm is summarized in Algorithm 1, which also includes the sampling-based approximation that we will describe in the next section.

Fig. 1 shows the approximation of the rational function in (4) sampled at 1001 points with a nonpassive model and a passive model using SOS polynomials. The nonpassive model provides an excellent match with an rms error in the order of 10^{-16}; however, it follows the nonpassive behavior of the original data. The passive model is obtained solving the semidefinite program in (14). The markers match the passivity violations as predicted by the passivity test based on roots. We ran the same example through the Matrix Fitting Toolbox, which implements passivity enforcement not only on scalars but also on multi-port network functions based on the perturbation of residue matrix eigenvalues [23]. The rms error of the passive model using SOS polynomials was 0.0190 compared to the higher error of 0.0265 of the perturbation-based approach. The error of the passive model using SOS polynomials was smaller than the perturbation approach in all examples discussed in this article, which is expected as a global minimum can be obtained in our approach by solving a convex optimization problem.

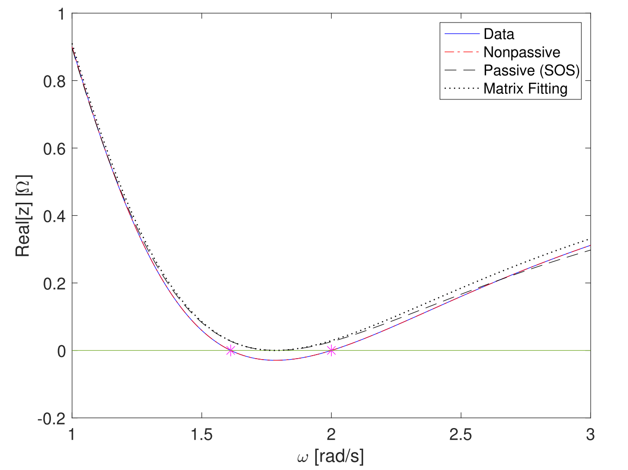

Fig. 1. Approximation of the rational function in (4) sampled at 1001 points (shown as data in the figure) with a nonpassive model, a passive model using SOS polynomials, and another passive model using the Matrix Fitting Toolbox [23]. The markers match the passivity violations as predicted by the passivity test based on roots.

Algorithm 1: Algorithm for Passive Scalar Function Approximation Using SOS Polynomials.

Input: strictly stable poles p_i, data $h(j\omega_i)$ at frequency points ω_i

Output: residue vector k, constant term d, linear term e of a passive rational function r in (1)

$k, d, e \leftarrow \min \sum_{i=0}^{M} |r(j\omega_i) - h(j\omega_i)|^2$
subject to $e \geq 0$ and the SOS constraint on $n(\omega^2)$ in (3) using
if coefficient-based optimization **then**
  the constraint in (13)
else if sampling-based optimization **then**
  the constraint in (15)
end if

The numerical conditioning of the problem due to the PSD constraint in (13) limits its use to low order models that have less than 10 poles in our tests. This is due to the poor conditioning of the semidefinite program that involves the coefficients of a monomial basis in SOS constraints. Next we present a modification of this method based on sampling to improve the numerical conditioning.

V. Sampling-Based Approximation Using SOS Polynomials

One way to avoid working directly with the coefficients of a monomial basis is to make use of the property that an nth degree polynomial is uniquely defined by sampling it at $n+1$ points [24], [25]. This brings a great advantage in solving (14) as we can remain in a partial-fractions basis without having to formulate the problem in terms of the monomial coefficients of $n(\omega^2)$.

Accordingly, a sampling-based formulation of the SOS constraint in (13) can be given as

$$d(\omega_j^2)\left(d+\sum_{i=0}^{N}\frac{-k_i p_i}{\omega_j^2+p_i^2}\right)$$
$$=[T_j]_p^T P[T_j]_p+(x_j-a)[T_j]_r^T R[T_j]_r,\ j=0,1,\ldots,N+1$$
$$P\succeq 0, R\succeq 0. \tag{15}$$

We can observe that the first line of (15) is equal to $n(\omega^2)$ evaluated at the sampling point $\omega^2=\omega_j^2$. We have the flexibility to have a different basis on both sides of this equation as the equality is in terms of the values and not coefficients. The right hand side are the samples of a nonnegative polynomial for $\omega^2\geq 0$ of the same degree. In the following, we use a scaled Chebyshev polynomial basis following [26] for the right hand side given by:

$$[T_j]_p^T=\sqrt{\frac{2}{2p+1}}[T_0(x_j)/\sqrt{2},T_1(x_j),\ldots,T_p(x_j)] \tag{16}$$

where T_j are Chebyshev polynomials of the first kind. This basis has good numerical properties, as it forms an orthonormal basis when sampled at Chebyshev points of the first kind

$$x_j=\cos\left(\frac{(j+1/2)\pi}{N+2}\right),\quad j=0,1,\ldots,N+1. \tag{17}$$

The frequency variable ω^2 on the left hand side is mapped to the Chebyshev nodes on the right hand side such that $\omega^2=0.5((\omega_{max}^2-\omega_{min}^2)x+(\omega_{max}^2+\omega_{min}^2))$. As a result, the inequality $\omega^2\geq 0$ is equivalent to $(x-a)\geq 0$ in (15), where $a=-(\omega_{max}^2+\omega_{min}^2)/(\omega_{max}^2-\omega_{min}^2)$.

VI. Numerical Examples

The first example is a pair of solid power/ground planes that have been simulated using the finite difference method [27] to obtain admittance parameters of two symmetrical ports. The power/ground planes in the simulation are square-shaped with a length of 4.8 mm on a side, separated by a dielectric having a dielectric constant of 4, thickness of 100 μm, and loss tangent of 0.02. Conductors are made of copper with a conductivity of 5.8×10^7 S/m. The two ports are placed on the diagonal, a quarter of a diagonal away from two opposite corners.

The input admittance data has nonpassive behavior in a small frequency range. Vector fitting was used to obtain a model with 30 stable poles after five iterations. The result was an excellent match to the provided data; therefore the outcome was also a nonpassive model. Next, the fifth iteration was replaced with the sampling-based SOS approach to obtain a passive model. Fig. 2 shows the comparison of the passive and nonpassive rational functions with the provided data.

The second example is a cavity resonator. The simulation is done using the full-wave simulator Sonnet [28] to obtain the input impedance of the resonator. Vector fitting provided

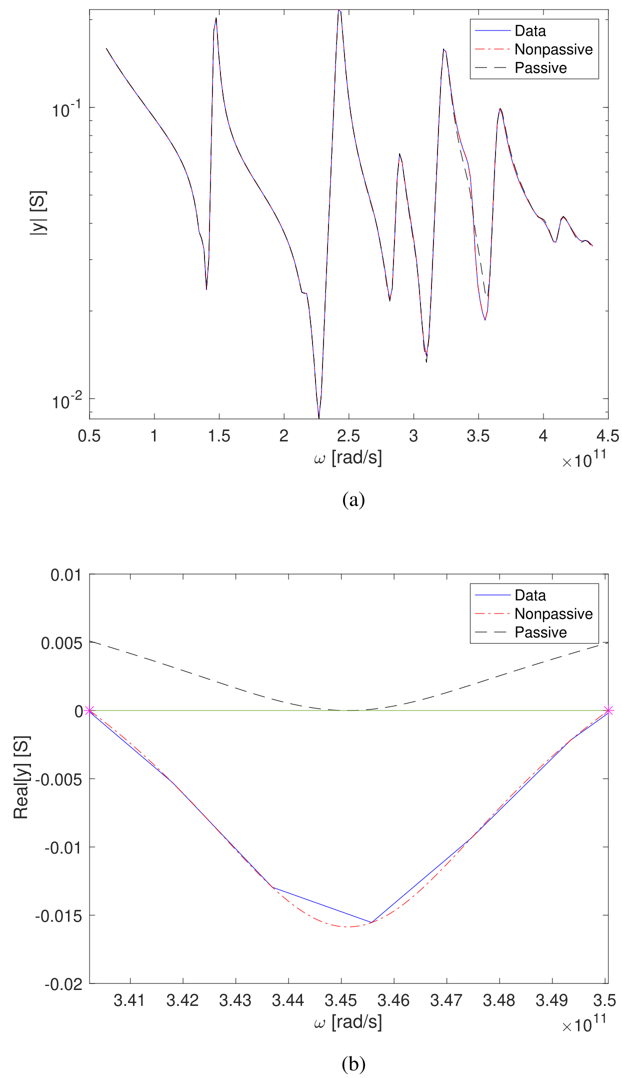

Fig. 2. (a) Magnitude and (b) zoomed-in real part of the input admittance of a pair of solid power/ground planes with two ports. Both the passive and nonpassive models have the same 30 poles. The markers match the passivity violations as predicted by the passivity test.

20 stable poles; however, the resulting model was nonpassive for $\omega>3.6820\times10^{11}$ rad/s. The initial model from sampling-based SOS method also did not result in a passive model. It was observed that the PSD constraint on the matrix P was not fulfilled as it contained a small negative eigenvalue with an amplitude that was smaller than the next smallest one by an order of 10^{-10}. This can be attributed to the termination criterion of the semidefinite program solver due to the floating-point arithmetic. To overcome this issue, the PSD constraint on P was enforced as $P\times 1000\succeq 0$, which resulted in a fully PSD Q and a passive model that provides an excellent match as shown in Fig. 3.

The final example is a common-mode filter for differential lines [29]. The measurement is done with a vector network analyzer to obtain admittance parameters of its four ports. Fig. 4 shows the comparison of the nonpassive model with ten poles with a passive model having the same poles. The nonpassive model had an rms error of 4.314, whereas the passive model

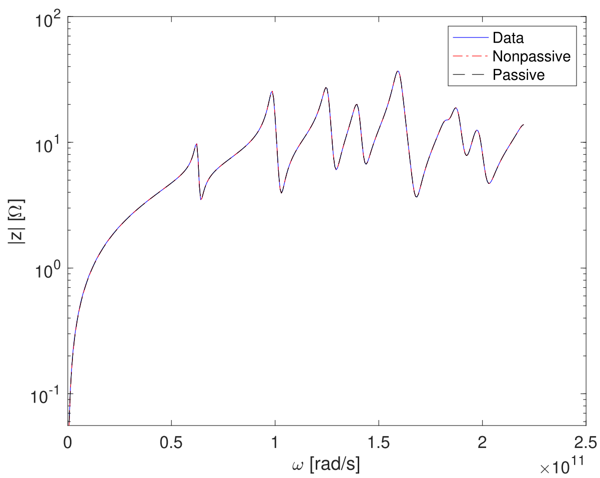

Fig. 3. Magnitude of the input impedance of a cavity resonator. Passivity violation for the nonpassive model occurs outside the frequency range of fitting for $\omega > 3.6820 \times 10^{11}$ rad/s.

had a slightly increased error of 4.316. The nonpassive model resulted in two frequency bands with passivity violations. The first band is within the frequency range of provided data as shown in Fig. 4(b). The second band is outside the data frequency range as shown in Fig. 4(c). The PSD constraint was enforced as $P \times 10 \succeq 0$ to correct an initial negative eigenvalue with an amplitude in the order of 10^{-9}.

A. Numerical Scaling

The numerical scaling is critical in setting up the semidefinite program. The following points provide a general strategy and the parameters used in the provided examples.

1) PSD constraints: PSD constraint on a matrix Q can be checked by ensuring all the eigenvalues are nonnegative. In some cases, the solver may terminate with eigenvalues that are negative but have very small amplitudes. The extracted model can then have a minimum for its real part that is negative but close to zero. If this is not acceptable, modifying the constraint so that $P \times a \succeq 0$ for an $a > 1$ can help enforce the PSD constraint also on eigenvalues with small amplitudes. In our tests, choosing $10 \leq a \leq 1000$ was sufficient to obtain a fully PSD matrix when there were initial small negative eigenvalues.
2) Norm minimization: In standard vector fitting, column scaling is applied on the system matrix to improve its condition number in solving the least-squares problem of fitting the residues [1], which can also be implemented in our passive modeling approach. In our tests, we simply normalized the frequency points with respect to the highest frequency.
3) Equality constraints: In solving the semidefinite program, the equality constraints are enforced within a tolerance [21]. This is critical as in (15) the equality constraints involve multiplication with $d(\omega_j^2)$, which can be very small. We normalized the equality constraints by the median value of $d(\omega_j^2)h_j$, where h_j is the real part of the data at frequency ω_j, obtained from a simple spline interpolation.
4) Sampling frequencies: The range for the sampling does not necessarily need to match the limits of the provided frequency points. In the given examples, we have used $\omega_{min}^2 = 0.1, \omega_{max}^2 = 0.9$ (after frequency normalization as discussed above).

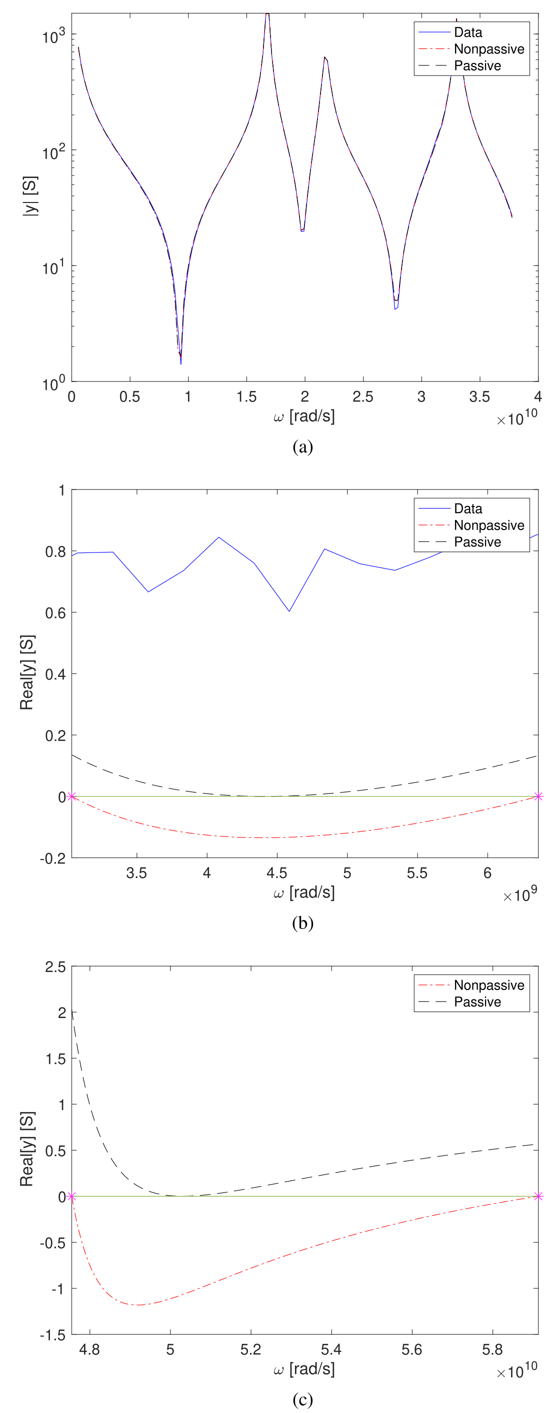

Fig. 4. (a) Magnitude and (b) zoomed-in real part of the measured input admittance of a common-mode filter at one of its four ports. The nonpassive model resulted in two frequency bands, (b) and (c), with passivity violations as shown.

VII. Conclusion

We introduced an intuitive passivity test based on the roots of the real part transfer function. This test provides a link between separate passivity tests applied based on the presence of a constant term in the pole-residue form. Based on this test, a sampling-based SOS algorithm was introduced for passive macromodeling to generate rational transfer functions from frequency responses available from simulated or measured data. Numerical examples have demonstrated that the method is able to find rational functions that accurately fit the data, while correcting any possible passivity violations in the provided data.

References

[1] B. Gustavsen and A. Semlyen, "Rational approximation of frequency domain responses by vector fitting," *IEEE Trans. Power Del.*, vol. 14, no. 3, pp. 1052–1061, Jul. 1999.

[2] A. Mayo and A. Antoulas, "A framework for the solution of the generalized realization problem," *Linear Algebra Appl.*, vol. 425, no. 2, pp. 634–662, 2007. [Online]. Available: https://www.sciencedirect.com/science/article/pii/S0024379507001280

[3] C. Sanathanan and J. Koerner, "Transfer function synthesis as a ratio of two complex polynomials," *IEEE Trans. Autom. Control*, vol. 8, no. 1, pp. 56–58, Jan. 1963.

[4] Y. Nakatsukasa, O. Sète, and L. N. Trefethen, "The AAA algorithm for rational approximation," *SIAM J. Sci. Comput.*, vol. 40, no. 3, pp. A1494–A1522, 2018. [Online]. Available: https://doi.org/10.1137/16M1106122

[5] I. V. Gosea and A. C. Antoulas, "Rational approximation of the absolute value function from measurements: A numerical study of recent methods," 2020, *arXiv:2005.02736*.

[6] J. E. Schutt-Aine *et al.*, "Comparative study of convolution and order reduction techniques for blackbox macromodeling using scattering parameters," *IEEE Trans. Compon. Packag. Manuf. Technol.*, vol. 1, no. 10, pp. 1642–1650, Oct. 2011.

[7] P. Triverio, S. Grivet-Talocia, M. S. Nakhla, F. G. Canavero, and R. Achar, "Stability, causality, and passivity in electrical interconnect models," *IEEE Trans. Adv. Packag.*, vol. 30, no. 4, pp. 795–808, Nov. 2007.

[8] B. Gustavsen, "Passivity assessment and enforcement utilizing eigenpairs information," *Elect. Power Syst. Res.*, vol. 194, 2021, Art. no. 107041. [Online]. Available: https://www.sciencedirect.com/science/article/pii/S0378779621000213

[9] S. Grivet-Talocia, "Passivity enforcement via perturbation of Hamiltonian matrices," *IEEE Trans. Circuits Syst. I: Regular Papers*, vol. 51, no. 9, pp. 1755–1769, Sep. 2004.

[10] S. Grivet-Talocia and A. Ubolli, "A comparative study of passivity enforcement schemes for linear lumped macromodels," *IEEE Trans. Adv. Packag.*, vol. 31, no. 4, pp. 673–683, Nov. 2008.

[11] L. De Tommasi, M. de Magistris, D. Deschrijver, and T. Dhaene, "An algorithm for direct identification of passive transfer matrices with positive real fractions via convex programming," *Int. J. Numer. Model.: Electron. Netw., Devices Fields*, vol. 24, no. 4, pp. 375–386, 2011. [Online]. Available: https://onlinelibrary.wiley.com/doi/abs/10.1002/jnm.784

[12] A. E. Engin, B. Adepu, M. Kusumoto, and T. Harada, "Macromodeling of complex power delivery networks for efficient transient simulation," in *Proc. IEEE CPMT Symp.*, 2012, pp. 1–4.

[13] A. Engin, "Passive multiport RC model extraction for through silicon via interconnects in 3-D ICS," *IEEE Trans. Electromagn. Compat.*, vol. 56, no. 3, pp. 646–652, Jun. 2014.

[14] B. D. O. Anderson and S. Vongpanitlerd, *Network Analysis and Synthesis*. Hoboken, NJ, USA: Prentice Hall, 1974.

[15] A. Semlyen and B. Gustavsen, "A half-size singularity test matrix for fast and reliable passivity assessment of rational models," *IEEE Trans. Power Del.*, vol. 24, no. 1, pp. 345–351, Jan. 2009.

[16] B. Gustavsen, "Improving the pole relocating properties of vector fitting," *IEEE Trans. Power Del.*, vol. 21, no. 3, pp. 1587–1592, Jul. 2006.

[17] R. Shorten, P. Curran, K. Wulff, and E. Zeheb, "A note on spectral conditions for positive realness of transfer function matrices," *IEEE Trans. Autom. Control*, vol. 53, no. 5, pp. 1258–1261, Jun. 2008.

[18] L. Knockaert, "A simple and accurate algorithm for barycentric rational interpolation," *IEEE Signal Process. Lett.*, vol. 15, pp. 154–157, 2008, doi: 10.1109/LSP.2007.913583.

[19] G. Blekherman, P. A. Parrilo, and R. R. Thomas, "Semidefinite optimization and convex algebraic geometry," G. Blekherman, P. A. Parrilo, and R. R. Thomas, Eds. Philadelphia, PA, USA: SIAM, 2012. [Online]. Available: https://epubs.siam.org/doi/abs/10.1137/1.9781611972290

[20] V. Powers and B. Reznick, "Polynomials that are positive on an interval," *Trans. Amer. Math. Soc.*, vol. 352, no. 10, pp. 4677–4692, 2000. [Online]. Available: http://www.jstor.org/stable/221758

[21] J. Lofberg, "Pre- and post-processing sum-of-squares programs in practice," *IEEE Trans. Autom. Control*, vol. 54, no. 5, pp. 1007–1011, May 2009.

[22] M. Grant and S. Boyd, "CVX: Matlab software for disciplined convex programming, version 2.1," 2014. [Online]. Available: http://cvxr.com/cvx

[23] B. Gustavsen, "Fast passivity enforcement for s-parameter models by perturbation of residue matrix eigenvalues," *IEEE Trans. Adv. Packag.*, vol. 33, no. 1, pp. 257–265, Feb. 2010.

[24] J. Lofberg and P. Parrilo, "From coefficients to samples: A new approach to sos optimization," in *Proc. 43rd IEEE Conf. Decis. Control*, 2004, vol. 3, pp. 3154–3159.

[25] E. de Klerk, G. Elabwabi, and D. den Hertog, "Optimization of univariate functions on bounded intervals by interpolation and semidefinite programming," *Oper. Res.*, CentER Discussion Paper 2006-26, Tilburg University, Tilburg, The Netherlands, Apr. 2006.

[26] D. Papp, "Semi-infinite programming using high-degree polynomial interpolants and semidefinite programming," *SIAM J. Optim.*, vol. 27, no. 3, pp. 1858–1879, 2017. [Online]. Available: https://doi.org/10.1137/15M1053578

[27] A. Engin, K. Bharath, and M. Swaminathan, "Multilayered finite-difference method (MFDM) for modeling of package and printed circuit board planes," *IEEE Trans. Electromagn. Compat.*, vol. 49, no. 2, pp. 441–447, May 2007.

[28] *Sonnet v16.56*. [Online]. Available: http://www.sonnetsoftware.com/

[29] W. A. Alarcon, A. E. Engin, I. Ndip, and K. Lang, "EBG common-mode filter design using uncoupled coplanar waveguide to microstrip transitions," *IEEE Lett. Electromagn. Compat. Pract. Appl.*, vol. 2, no. 3, pp. 81–84, Sep. 2020.

Arif Ege Engin (Member, IEEE) received the B.S. degree in electrical engineering from Middle East Technical University, Ankara, Turkey, in 1998, the M.S. degree in electrical engineering from the University of Paderborn, Paderborn, Germany, in 2001, and the Ph.D. degree from the University of Hannover, Hanover, Germany, in 2004.

He worked as a Research Engineer with the Fraunhofer-Institute for Reliability and Microintegration, Berlin, Germany. From 2006 to 2008, he was an Assistant Research Director with Microsystems Packaging Research Center, Georgia Tech. He is currently a Professor with the Electrical and Computer Engineering Department, San Diego State University, San Diego, CA, USA. He has authored and coauthored more than 100 publications in journals and conferences in the areas of signal and power integrity modeling and simulation and four patents. He is the co-author of the book Power Integrity Modeling and Design for Semiconductors and Systems, translated to Japanese and Chinese.

Dr. Engin was the recipient of the Semiconductor Research Corporation Inventor Recognition Award in 2009, the Outstanding Educator Award from the International Microelectronics Packaging and Assembly Society in 2015, the Alexander-von-Humboldt Research Fellowship for 2015 and 2018, and the 2017 IEEE EMC-S M. Kanda Award for the Most Cited Paper in the last five years (2013–2017).